

# Quantum Teleportation with Atoms Trapped in Cavities

Jaeyoon Cho and Hai-Woong Lee

Department of Physics, Korea Advanced Institute of Science and Technology, Daejeon 305-701, Korea

(Dated: May 6, 2019)

We propose a scheme to implement the quantum teleportation protocol with single atoms trapped in cavities. The scheme is based on the adiabatic passage and the polarization measurement. We show that it is possible to teleport the internal state of an atom trapped in a cavity to an atom trapped in another cavity with the success probability of 1/2 and the fidelity of 1. The scheme is resistant to a number of considerable imperfections such as the violation of the Lamb-Dicke condition, weak atom-cavity coupling, spontaneous emission, and detection inefficiency.

Recent advances in cavity quantum electrodynamics made it possible to trap and manipulate single atoms in high- $Q$  cavities [1, 2] and thereby to achieve various modes of quantum information processing with single trapped atoms. There have been numerous proposals to use single trapped atoms for quantum information processing, such as for entanglement generation [3], quantum computation [4], quantum communication [5], and for quantum teleportation [6], the topic of our present investigation.

Since the first proposal [7], quantum teleportation of polarization states of single photons and squeezed states of light has been demonstrated experimentally [8]. Experimental demonstration of teleportation of atomic states, however, is yet to be realized. In earlier proposals of quantum teleportation of atomic states [9], qubits were internal states of single flying atoms. From the viewpoint of quantum information processing, however, it would be ideal to have atoms as stationary qubits used only for storage of information and leave communication to photons. The above mentioned advances in cavity quantum electrodynamics techniques of trapping and manipulating atoms open ways for such a scheme.

In Ref. [6], Bose *et al.* suggested a scheme for quantum teleportation with two  $\Lambda$ -type three-level atoms each trapped in a cavity, where photons leaking out from the cavities are used for Bell measurement. In the preparation stage, Alice maps her unknown atomic state into her cavity mode state, while Bob entangles his atomic state with his cavity mode state. Photons leaking out from both cavities interfere at a 50-50 beam splitter at Alice's site. If only one photon has been detected during a definite measurement period, Alice comes to the conclusion that the Bell measurement has been succeeded. Although the scheme is comparatively easy to implement, it has the following disadvantages: 1) Since the preparation takes time and succeeds only when no photon leaks out during the preparation period, the loss of the success probability is unavoidable. 2) The Bell measurement is incomplete in that there remains the possibility that one more photon leaks out after the detection of one photon during the measurement period. This results in the loss of the fidelity. 3) The detectors have to be able to distinguish between different numbers (one and two) of photons.

In this letter, we propose a scheme to implement quantum teleportation with single trapped atoms. The basic idea of the scheme is similar to that of Bose *et al.*, so that it inherits the simplicity of their scheme, whereas with our scheme both the success probability of 1/2 and the fidelity of 1 can be achieved. Moreover our scheme does not require distinguishing between one and two photons.

The schematic representation of our scheme is shown in Fig. 1. The atom A is trapped in Alice's cavity, and the atom B in Bob's cavity. Each atom is driven adiabatically by a classical coherent field. The level structures of atoms will be described later. Alice maps the unknown internal state of her atom into the two-mode state of her cavity through adiabatic passage, while Bob generates a maximally entangled state of the internal state of his atom and the two-mode state of his cavity through adiabatic passage. During both the adiabatic passage processes, with the probability of 1, each cavity should emit one photon with two possible polarization degrees of freedom in which the quantum information is encoded. Two photons leaking out from both cavities interfere at the 50-50 beam splitter S. The beam splitter S, two quarter wave plates  $W_1$  and  $W_2$ , two polarization beam

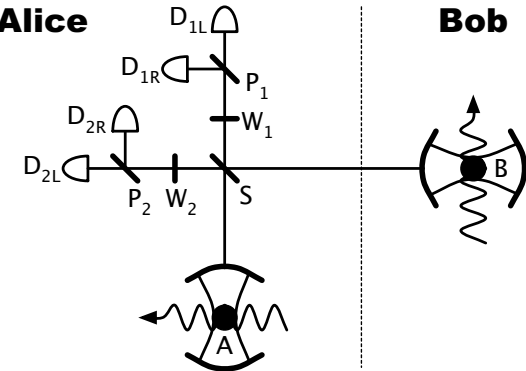


FIG. 1: Experimental scheme to teleport the internal state of atom A to atom B. S is a beam splitter,  $W_1$  and  $W_2$  are quarter wave plates,  $P_1$  and  $P_2$  are polarization beam splitters, and  $D_{1L}$ ,  $D_{2L}$ ,  $D_{1R}$ , and  $D_{2R}$  are photodetectors. Each winding arrow represents the classical driving field

splitters  $P_1$  and  $P_2$ , and four detectors  $D_{1L}$ ,  $D_{1R}$ ,  $D_{2L}$ , and  $D_{2R}$  constitute a measurement device for discriminating between the Bell states of the two single-photon polarization qubits.

The involved atomic levels and transitions are depicted in Fig. 2. For the operation, both Alice and Bob exploit two  $F = 1$  hyperfine levels, whereas Bob exploits one additional hyperfine level. A qubit is encoded in two Zeeman sublevels of the  $F = 1$  ground hyperfine level. To express the state of the atom-cavity system, we use the notation

$$|\Psi(t)\rangle_i = |x\rangle_i |n_L, n_R\rangle_i, \quad (1)$$

where  $i = A, B$  denotes Alice or Bob,  $x$  the atomic state, and  $n_{L,R}$  the number of left- or right-circularly polarized photons in Alice's or Bob's cavity. Transitions between the  $F = 1$  ground and excited hyperfine levels, both the cavity modes, and the classical field for Alice are all resonant with the same frequency  $\omega$ , whereas the transition  $|g'_0\rangle_B \leftrightarrow |e_0\rangle_B$  and the classical field for Bob are resonant with another frequency  $\omega'$ .  $\Omega_i(t)$  and  $g_i$  represent the time-dependent Rabi frequency of the classical field (assumed to be real without loss of generality) and the atom-cavity coupling rate (assumed to be the same for both the transitions) respectively, with  $i = A, B$  for Alice or Bob. For the moment, we assume that  $g_i$  remains

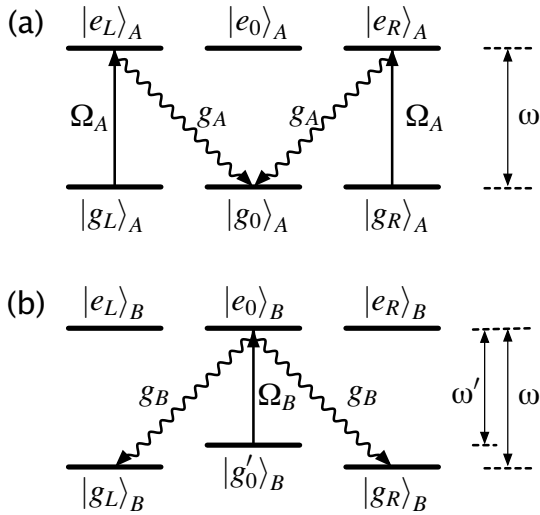


FIG. 2: The involved atomic levels and transitions for Alice (a) and Bob (b). Alice's qubit is encoded in the two Zeeman sublevels  $|g_L\rangle_A$  and  $|g_R\rangle_A$ , and Bob's qubit in the same way. Each straight arrow represents the transition driven by the  $\pi$ -polarized classical coherent field and each winding arrow represents the transition due to the atom-cavity coupling. Each transition of  $|e_L\rangle_A \rightarrow |g_0\rangle_A$  and  $|e_0\rangle_B \rightarrow |g_R\rangle_B$  ( $|e_R\rangle_A \rightarrow |g_0\rangle_A$  and  $|e_0\rangle_B \rightarrow |g_L\rangle_B$ ) is coupled to the left-circularly (right-circularly) polarized mode of the cavity. The transition  $|g_0\rangle_A \leftrightarrow |e_0\rangle_A$  is electric dipole forbidden.  $\omega$  and  $\omega'$  represent the relevant transition frequencies.

constant during the operation. The assumption is valid in the Lamb-Dicke limit. The effect of time-varying  $g_i$  will be discussed later.

Initially, Alice's system is prepared in the following state:

$$|\Psi(0)\rangle_A = (\alpha |g_L\rangle + \beta |g_R\rangle)_A |0,0\rangle_A, \quad (2)$$

where  $\alpha$  and  $\beta$  are unknown. If the variation of  $\Omega_A(t)$  is sufficiently slow, only the four transitions are involved as depicted in Fig. 2(a):  $|g_m\rangle_A \rightarrow |e_m\rangle_A$  ( $m = L, R$ ) driven by the  $\pi$ -polarized classical field and  $|e_L\rangle_A \rightarrow |g_0\rangle_A$  ( $|e_R\rangle_A \rightarrow |g_0\rangle_A$ ) coupled to the left-circularly (right-circularly) polarized mode of the cavity. The transition between  $|g_0\rangle_A$  and  $|e_0\rangle_A$  is electric dipole forbidden. Consequently, in the rotating frame, the Hamiltonian of the total system can be written as

$$H_A = \Omega_A(t)(|e_L\rangle \langle g_L| + |e_R\rangle \langle g_R|)_A + g_A(a_L^A |e_L\rangle \langle g_0| + a_R^A |e_R\rangle \langle g_0|)_A + h.c., \quad (3)$$

where  $a_{L,R}^A$  denotes the annihilation operator for the corresponding polarized mode of the cavity. The dark space is spanned by the two eigenstates  $|D_1(t)\rangle_A = \cos \theta_A(t) |g_L\rangle_A |0,0\rangle_A - \sin \theta_A(t) |g_0\rangle_A |1,0\rangle_A$  and  $|D_2(t)\rangle_A = \cos \theta_A(t) |g_R\rangle_A |0,0\rangle_A - \sin \theta_A(t) |g_0\rangle_A |0,1\rangle_A$ , where  $\theta_A(t)$  is given by  $\cos \theta_A(t) = \frac{g_A}{\sqrt{|g_A|^2 + |\Omega_A|^2}}$  and  $\sin \theta_A(t) = \frac{\Omega_A(t)}{\sqrt{|g_A|^2 + |\Omega_A|^2}}$ . In the adiabatic limit, the initial state (2) evolves in the dark space into the following state:

$$\begin{aligned} |\Psi(t)\rangle_A &= \alpha |D_1(t)\rangle_A + \beta |D_2(t)\rangle_A \\ &= \cos \theta_A(t) (\alpha |g_L\rangle + \beta |g_R\rangle)_A |0,0\rangle_A \\ &\quad - \sin \theta_A(t) |g_0\rangle_A (\alpha |1,0\rangle + \beta |0,1\rangle)_A. \end{aligned} \quad (4)$$

Alice, thus, can map her atomic state  $(\alpha |g_L\rangle + \beta |g_R\rangle)_A$  into her cavity mode state  $(\alpha |1,0\rangle + \beta |0,1\rangle)_A$  by simply increasing  $\sin \theta_A(t)$  adiabatically.

For Bob, the atom is initially prepared in the state  $|g'_0\rangle_B |0,0\rangle_B$ . The process for Bob is similar to that for Alice. With  $\Omega_B$  varied adiabatically, only the three transitions are involved as depicted in Fig. 2(b):  $|g'_0\rangle_B \rightarrow |e_0\rangle_B$  driven by the  $\pi$ -polarized classical field and  $|e_0\rangle_B \rightarrow |g_L\rangle_B$  ( $|e_0\rangle_B \rightarrow |g_R\rangle_B$ ) coupled to the right-circularly (left-circularly) polarized mode of the cavity. Consequently, in the rotating frame, the Hamiltonian of the total system can be written as

$$H_B = \Omega_B(t)(|e_0\rangle \langle g'_0|)_B + g_B(a_R^B |e_0\rangle \langle g_L| + a_L^B |e_0\rangle \langle g_R|)_B + h.c., \quad (5)$$

where  $a_{L,R}^B$  denotes the annihilation operator for the corresponding polarized mode of the cavity. In the adiabatic limit, the initial state evolves into the following dark state:

$$\begin{aligned} |\Psi(t)\rangle_B &= \cos \theta_B(t) |g'_0\rangle_B |0,0\rangle_B - \\ &\quad \sin \theta_B(t) \frac{|g_L\rangle_B |0,1\rangle_B + |g_R\rangle_B |1,0\rangle_B}{\sqrt{2}}, \end{aligned} \quad (6)$$

where  $\theta_B(t)$  is given by  $\cos\theta_B(t) = \frac{\sqrt{2}g_B}{\sqrt{2|g_B|^2+|\Omega_B|^2}}$  and  $\sin\theta_B(t) = \frac{\Omega_B(t)}{\sqrt{2|g_B|^2+|\Omega_B|^2}}$ . Bob also increase  $\sin\theta_B(t)$  adiabatically to generate a maximally entangled state  $\frac{(|g_L\rangle|0,1\rangle+|g_R\rangle|1,0\rangle)_B}{\sqrt{2}}$ .

As  $\sin\theta_A(t)$  and  $\sin\theta_B(t)$  are increased, each cavity emits one photon at some instant. To illustrate the basic idea of our scheme, let us first assume that both the photons reach simultaneously at the beam splitter  $S$ . Expressing the polarizations of each photon as  $|L\rangle_i$  and  $|R\rangle_i$  respectively, with  $i = A, B$  for Alice or Bob, the total state can be written as

$$|\Psi'\rangle = \frac{1}{\sqrt{2}} |g_0\rangle_A (\alpha |L\rangle + \beta |R\rangle)_A (|R\rangle |g_L\rangle + |L\rangle |g_R\rangle)_B. \quad (7)$$

Now it is clear that a Bell measurement with two single-photon polarization qubits followed by the corresponding unitary operation to Bob's atom completes the quantum teleportation. As we consider only linear optical elements, the success probability of such a Bell measurement has been limited up to 1/2 [10]. Our scheme also succeeds with that probability. In our setup of Fig. 1, the Bell measurement succeeds only when the two photons are found to be oppositely polarized at two detectors. From simple calculations, it is found that when  $D_{1L}$  and  $D_{1R}$  click or  $D_{2L}$  and  $D_{2R}$  click, the state of Bob's atom collapses into the state  $\alpha |g_L\rangle_B + \beta |g_R\rangle_B$ , whereas when  $D_{1L}$  and  $D_{2R}$  click or  $D_{2L}$  and  $D_{1R}$  click, into the state  $\alpha |g_L\rangle_B - \beta |g_R\rangle_B$ . For the latter case, Bob applies an appropriate local unitary operation to his atom to transform the state into the former one.

We return to the actual situation in which each photon

leaks out from the cavity in the form of a single-photon pulse due to the random nature of the emission. In the adiabatic limit, the pulse shape can be calculated as [11]

$$f_i(t) = \sqrt{\kappa_i} \sin\theta_i(t) \exp\left(-\frac{\kappa_i}{2} \int_0^t \sin^2\theta_i(\tau)d\tau\right), \quad (8)$$

where  $\kappa_i$  denotes the cavity decay rate for Alice ( $i = A$ ) or Bob ( $i = B$ ). The pulse shape function  $f_i(t)$  is normalized so that  $\int_0^\infty |f_i(t)| dt = 1$ . The two photons interfere maximally when the two pulse shapes overlap completely at the beam splitter. Therefore, in order to get the maximum fidelity of 1,  $\Omega_i(t)$  should be adjusted to satisfy  $\sin\theta_A(t) = \sin\theta_B(t)$ , where we have assumed that two distances between the cavities and the beam splitter are the same. We do not have to adjust the exact pulse shape. From a simple algebra, we obtain the following condition:

$$\Omega_B(t) = \sqrt{2} \frac{g_B}{g_A} \Omega_A(t). \quad (9)$$

In the remainder, we consider effects of imperfections which could arise in a realistic implementation. First we consider the problem related to the Lamb-Dicke limit. So far we have assumed that  $g_i$  is a constant. However, when the Lamb-Dicke condition is not fulfilled  $g_i$  varies in time. The change of  $g_i$  is accompanied with the change of the output pulse shape  $f_i(t)$ . From a straightforward calculation, the fidelity of the resulting state of Bob's atom with respect to the initial state of Alice's atom can be derived as

$$F = \sqrt{A\langle\Psi(0)|\rho_B|\Psi(0)\rangle_A} = \sqrt{|\alpha|^4 + |\beta|^4 + 2|\alpha\beta|^2 \operatorname{Re} \left[ \int_0^\infty dt_1 \int_0^\infty dt_2 f_A^*(t_1) f_B(t_1) f_B^*(t_2) f_A(t_2) \right]}, \quad (10)$$

where  $\rho_B$  denotes Bob's state. Noting that  $\Omega_i(t)$  is assumed to be real, we obtain a simpler form of the fidelity depending on the overlap of the two pulse shapes as the following:

$$F = \sqrt{|\alpha|^4 + |\beta|^4 + 2|\alpha\beta|^2 \left[ \int_0^\infty f_A(t) f_B(t) dt \right]^2}. \quad (11)$$

To give a typical value of  $F$ , we consider a more specific situation in which each atom is placed inside a far-off resonance trapping (FORT) potential [2]. A FORT beam generates multiple potential wells along the cavity axis, and each potential well gives rise to a different value of the atom-cavity coupling rate. For simplicity,

we assume that each atom is trapped in the same potential well. From now on we take the parameters and the results of the numerical simulations of Ref. [12] as a typical example. Noting that the atomic motion in radial direction is too small to affect the atom-cavity coupling rate, we approximate the time-dependence of  $g_i$  as  $g_i(t) = g_{i0} \sin[2\pi(1.5 + 0.15 \sin(\omega_i^z t + \phi_i))]$ , where  $g_{i0}$  and  $\omega_i^z$  denote the maximum value of  $g_i(t)$  and the oscillation frequency of the atom along the cavity axis, respectively. Here, we have introduced an arbitrary phase  $\phi_i$ . The classical field that we consider is of the Gaussian form:  $\Omega_i(t) = \Omega_{i0} \exp\left[-\left(\frac{t-t_c}{\Delta t}\right)^2\right]$ , where  $t_c = 15 \mu\text{s}$  and  $\Delta t = 4 \mu\text{s}$ . We choose the parameters according

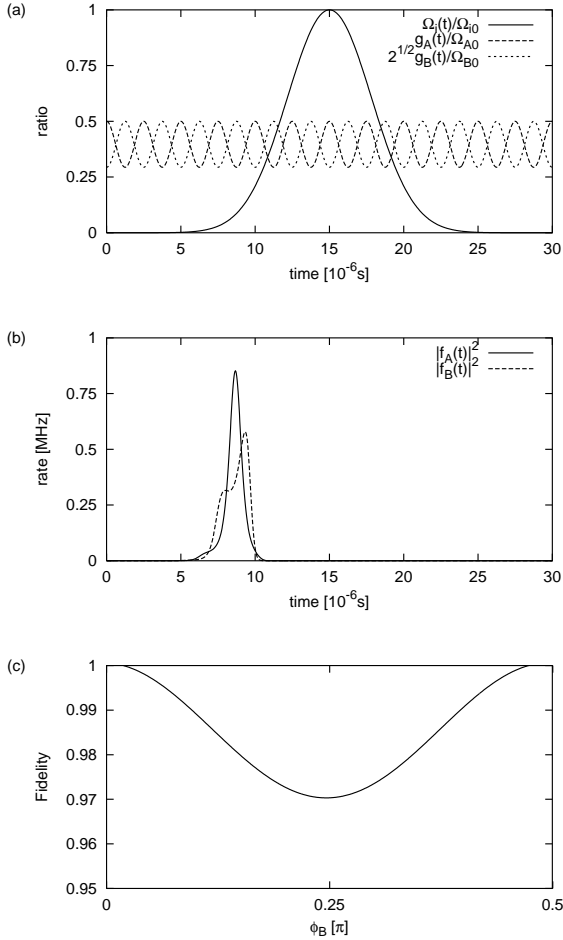


FIG. 3: Numerical simulations for a typical case: (a) Classical input pulses and time-varying atom-cavity coupling rates. (b) Pulse shapes of single photons leaking out from the cavities. (c) Fidelity with respect to  $\phi_B$ .

to Ref. [12] and the condition (9) as:  $\kappa_i/2\pi = 4$  MHz,  $\omega_i^z/2\pi = 0.2$  MHz,  $\Omega_{A0} = 2g_{A0}$  and  $\Omega_{B0} = 2\sqrt{2}g_{B0}$ . With these parameters the variations of the classical fields and the atom-cavity coupling rates are plotted in Fig. 3(a), where we have chosen two arbitrary phases as  $\phi_A = 0$  and  $\phi_B = \pi/4$ . In this condition the two atomic motions are out of phase, thus the fidelity is lowest due to the minimum overlap of the output pulse shapes. We have simply integrated Eq. (8) to get the pulse shapes. They are plotted in Fig. 3(b). In Fig. 3(c), we plot the fidelity with respect to  $\phi_B$  while fixing  $\phi_A$  as zero. It has been obtained by substituting Eq. (8) into Eq. (11) and integrating Eq. (11). Here, we have chosen the state to be teleported as  $|\Psi(0)\rangle_A = \frac{|g_L\rangle_A + |g_R\rangle_A}{\sqrt{2}}$ . In fact, this initial state gives rise to the lowest fidelity. Even in this case, however, Fig. 3(c) shows that the quantum teleportation is performed with a very high fidelity.

The advantages of our scheme become more obvious

when we further consider other possible imperfections. First of all, our scheme does not need to be operated in the strong atom-cavity coupling regime  $g_i^2/\kappa_i\gamma \gg 1$ , where  $\gamma$  is the spontaneous decay rate of the atom. The reason is that our scheme makes use of cavity decays for the interference effect, which is essential for the Bell measurement. Moreover the spontaneous decay of the atom does not have a critical effect on our scheme since the atomic state evolves in the ground dark space which does not couple to the excited hyperfine level. Besides, our scheme is designed so that the number of photons leaking out from the cavities is fixed as two and the quantum teleportation is completed only when two photons are detected at two different detectors. Therefore the detection efficiency does not affect the fidelity (when we ignore dark counts) and photon-counting detectors are not needed. Low detection efficiency lowers only the success probability.

Finally, we suggest <sup>87</sup>Rb as a good candidate for experimental realization of our scheme. As applied to our scheme, the states (<sup>5</sup>S<sub>1/2</sub>,  $F = 1$ ) and (<sup>5</sup>P<sub>3/2</sub>,  $F = 1$ ) of <sup>87</sup>Rb correspond to the  $F = 1$  ground and excited hyperfine levels we considered, respectively, and the state (<sup>5</sup>S<sub>1/2</sub>,  $F = 2, m = 0$ ) corresponds to  $|g'_0\rangle_B$ . Since the atomic properties of rubidium are similar to those of cesium considered in Ref. [2], we expect that rubidium can also be trapped at the single-atom level with far-off resonance trapping within the current technology.

---

- [1] J.M. Raimond *et al.*, Rev. Mod. Phys. **73**, 565 (2001) and references therin.
- [2] J. Ye *et al.*, Phys. Rev. Lett. **83**, 4987 (1999); J. McKeeever *et al.*, Phys. Rev. Lett. **90**, 133602 (2003).
- [3] J. Hong *et al.*, Phys. Rev. Lett. **89**, 237901 (2002); A.S. Sørensen *et al.*, Phys. Rev. Lett. **90**, 127903 (2003); X.-L. Feng *et al.*, Phys. Rev. Lett. **90**, 217902 (2003).
- [4] T. Pellizzari *et al.*, Phys. Rev. Lett. **75**, 3788 (1995).
- [5] J.I. Cirac *et al.*, Phys. Rev. Lett. **78**, 3221 (1997); T. Pellizzari, Phys. Rev. Lett. **79**, 5242 (1997).
- [6] S. Bose *et al.*, Phys. Rev. Lett. **83**, 5158 (1999).
- [7] C.H. Bennett *et al.*, Phys. Rev. Lett. **70**, 1895 (1993).
- [8] D. Bouwmeester *et al.*, Nature **390**, 575 (1997); D. Boschi *et al.*, Phys. Rev. Lett. **80**, 1121 (1998); A. Furusawa *et al.*, Science **282**, 706 (1998).
- [9] L. Davidovich *et al.*, Phys. Rev. A **50**, R895 (1994); J.I. Cirac and A.S. Parkins, Phys. Rev. A **50**, R4441 (1994); M.H.Y. Moussa, Phys. Rev. A **55**, R3287 (1997); S.B. Zheng and G.C. Guo, Phys. Lett. A **232**, 171 (1997); N.G. Almeida *et. al.*, Phys. Lett. A **241**, 213 (1998); S.B. Zheng, Opt. Commun. **167**, 111 (1999).
- [10] N. Lütkenhaus, J. Calsamiglia, and K.-A. Suominen, Phys. Rev. A **59**, 3295 (1999).
- [11] L.-M. Duan *et al.*, Phys. Rev. A **67**, 032305 (2003).
- [12] S.J. van Enk *et al.*, Phys. Rev. A **64**, 013407 (2001).